Synthesis and Characterization of Human Skin-Compatible Conductive Flexible Cellulose Carbon Nanohorn Sheets

Karthik Paneer Selvam
 Okayama Daigaku

Taichi Nagahata
 Okayama Daigaku

Kosuke Kato
 Okayama Daigaku

Mayuko Koreishi
 Okayama Daigaku

Toshiyuki Nakamura
 Okayama Daigaku

Yoshimasa Nakamura
 Okayama Daigaku

Takeshi Nishikawa
 Okayama Daigaku

Ayano Satoh
 Okayama Daigaku

Yasuhiko HAYASHI
 Okayama Daigaku

Research article

Keywords: Carbon Nanohorns, Cellulose, Skin Sensitization, Composites, Bio-compatible

Abstract

Background: Conductive sheets of cellulose and carbon nanomaterials and its human skin applications are an interesting research aspect as they have potential for applications for skin compatibility. Hence it is needed to explore the effects and shed light on these applications.

Method: To fabricate wearable, portable, flexible, lightweight, inexpensive, and biocompatible composite materials, carbon nanohorns (CNHs) and hydroxyethylcellulose (HEC) were used as precursors to prepare CNH-HEC (Cnh-cel) composite sheets. Cnh-cel sheets were prepared with different loading concentrations of CNHs (10, 20 50,100 mg) in 200 mg cellulose. To fabricate the bio-compatible sheets, a pristine composite of CNHs and HEC was prepared without any pretreatment of the materials.

Results: The obtained sheets are conductive (1.83×10^{-5} S) and bio-compatible with human skin. Analysis for skin-compatibility was performed for Cnh-cel sheets by h-CLAT *in vitro* skin sensitization tests to evaluate the activation of THP-1 cells. It was found that THP-1 cells were not activated by Cnh-cel; hence Cnh-cel is a safe biomaterial for human skin. It was also found that the composite allowed only a maximum loading of 100 mg to retain the consistent geometry of free-standing sheets of < 100 µm thickness. Since CNHs have a unique arrangement of aggregates (dahlia structure), the composite is homogeneous, as verified by transmission electron microscopy (TEM) and, scanning electron microscopy (SEM), and other functional properties investigated by Raman spectroscopy, Fourier transform infrared spectroscopy (FT-IR), conductance measurement, tensile strength measurement, and skin sensitization.

Conclusion: It can be concluded that cellulose and CNHs sheets are conductive and compatible to human skin applications.

Introduction

Among all the nanomaterials, carbon nanomaterials exhibit the most unique properties. Many prominent applications involving materials synthesized with carbon nanomaterials have gained popularity in recent years. Owing to their unique geometry, and properties closely related to single-walled carbon nanotubes (SWCNTs), carbon nanohorns (CNHs) have attracted significant attention. However, CNHs have different profiles of dispersion, structural geometry, surface chemistry, and synthesis methods and hence have a different properties. The toxicity of carbon nanomaterials is also a significant limitation for bio-related applications. Many metals are used as catalysts for the synthesis of carbon nanotubes (CNT) and other carbon nanomaterials (1). Owing to the inter-wall attraction force (van der Waals) of the CNTs, the dispersion of CNTs is a cumbersome process, and harsh chemical treatments using acids, and surfactants are necessary (2, 3).

CNHs may be an effective alternative to CNTs because they exhibit excellent purity and does not require post-synthesis treatment. CNHs have horn-shaped capped ends of approximately 2–3 nm, the wider ends aggregate to other CNHs, resulting in a Dahlia-like spherical structure (4). The void between the tips of adjacent CNHs allows the CNH aggregates to have an active dispersion profile compared to CNTs.

Although functionalization improved CNHs dispersion, the CNH aggregates could not be separated into single CNHs by chemical functionalization (5). The three-dimensional arrangement of the CNHs aggregates allows electron transport and influences the bonding within the polymer along the surface, enhancing the mechanical properties of the composite, compared to the one-dimensional confinement of CNTs. Research on oxidized CNHs to entrap anticancer agents to treat lung cancer was reported as early as 2005 (6). Polymer composites comprising poly-(vinyl alcohol), graphene, and CNHs have also been reported recently (7).

On the other hand, cellulose is an abundantly available natural polymer (8). In particular, Hydroxyethylcellulose (HEC) is a derived cellulose that is used as a thickening agent, which are widely used materials in industries. HEC is also known for its application in the pharmaceutical industry for capsule formulations to improve hydrophilization of drugs (9). Research on cellulose composites with carbon nanomaterials has been increasingly, with multiple reports on the numerous applications of cellulose-carbon nanomaterials. CNTs and cellulose composites have recently been studied as aerogels for vapor sensing (10) and, water sensors (11). In addition, graphene oxide coated with cellulose nanofibers have been used for designing transparent conductive paper (12). A few other have reports included the doping of conductive nanomaterials such as Ag nanowires, for electromagnetic interference shielding (13) and, PEDOT: PSS/MWCNT for supercapacitor electrodes (14).

In the area of smart, bio-compatible, wearable devices carbon nanomaterials are being widely researched. To accommodate a device in close contact with human body/skin the compatibility of the material is a very crucial aspect. To evaluate allergic reactions and safety of different materials to human skin, will help in further exploring different applications of new materials. Such as, allergic dermatitis caused by skin sensitizers is one of the prominent items safety compliance considerations. To evaluate the skin sensitization potential of the prepared Cnh-cel sheets, h-CLAT, an *in vitro* skin sensitization test [including cytotoxicity test] was carried out. The cytotoxicity of CNH is expected to be low because of its spherical aggregates, as no metal catalyst is used during the synthesis of CNHs. CNHs and their composite materials are applicable to living bodies, especially in the medical field, safety evaluations, such as those evaluating toxicity and allergy, are strictly tested and regulated for safety.

For the safety evaluation of substances, allergic dermatitis is one of the essential items. After skin contact, substances causing allergic reactions, such as rash, are termed skin sensitizers, and the processes causing allergic reactions are termed skin sensitization (GHS 2017). The mechanisms of skin sensitization have been summarized in the form of an adverse outcome pathway (AOP) ranging from early events at the molecular level to adverse events through intermediate events, including the following four events (OECD 2014) (16). The first event is the formation of covalent bonds between the electrophile; in other words, skin sensitizers covalently bind to the nucleophilic center of the proteins present in the skin. The second event includes inflammatory reactions, particularly in the keratinocytes in the skin, activation of the antioxidants/electrophilic substance responsive element (AREs) dependent signal transduction pathways. The third event is the activation of antigen-presenting cells called dendritic cells in the immune system, which is assessed by the expression of specific cell surface markers, chemokines,

and cytokines. The fourth event is the proliferation of T cells, which play a central role in the host immune response. The evaluation of skin sensitization using animal (*in vivo*) and non-animal (*in vitro*) experiments aims to reproduce all or part of the AOP. *In vivo* animal experiments include guinea pig maximization (OECD 1992) (17) and the mouse regional lymph node test (OECD 2010) (18).

From the viewpoint of animal protection, regulations on animal experiments have become stricter in recent years. Particularly in the cosmetic industry in the EU, animal experiments for the production and evaluation of raw materials, processed products, and final products, have been banned (Ban on animal testing 2019). Additionally, sales and imports of such materials and products have also been banned; therefore, manufacturers exporting these to the EU are forced to comply. Thus, non-animal tests for the evaluation of skin sensitization are necessary. Currently, peptide binding tests (the first event of AOP) (DPRA 2019, OECD 2019; Gerberick et al. 2004, 2007), keratinocyte reporter assay (the second event of AOP) (24−28), and human cell line activation test h-CLAT (the third event of AOP) are available and have been summarized in the OECD test guidelines as alternative evaluation methods (OECD, 2015a(22); OECD, 2015b(28); OECD, 2016 (29)).

The h-CLAT is a test method to evaluate the third event of the AOP by measuring the expression level of the cell surface marker (OCED, 2016) (30). It is known that upon the activation of dendritic cells, the expression levels of cell surface markers such as CD86 and CD54 increase also (31). In h-CLAT, the human monocytic leukemia cell line THP-1 cells were used as the dendritic cell model to evaluate the ability of test substances to activate dendritic cells.

In this study, we aimed to evaluate skin sensitization and cytotoxicity of novel composites of CNH and cellulose sheets using h-CLAT. These Cnh-cel sheets enabled the application of the novel composites in the field of restricted animal experiments.

Materials

Hydroxyethylcellulose (HEC) from Wako chemicals, Carbon nanohorns (CNHs) prepared by submerged arc discharge method over 90% purity, deionized (DI) water from Wako chemicals were used for the preparation of cnh-cel sheets. For performing skin sensitization tests, THP-1 cells RCB1189, Riken, RBC, Tsukuba, Japan, RPMI-1640 medium from Nakalai Tesuque, Kyoto, Japan, fetal bovine serum (FBS) form Nichirei Biosciences, Tokyo, Japan, mM 2-mercaptoethanol, streptomycin both from Nakalai Tesuque are used. Also, human globulin Cohn fraction II, III from Sigma-Aldrich, St. Louis, MO. Antibodies, anti-CD86 BD-PharMingen, Franklin Lakes, NJ, anti-CD54 or mouse IgG 1 both from Dako, Santa Clara, CA were used.

Methods

Cnh-cel sheet synthesis

Hydroxyethylcellulose, carbon nanohorns, and deionized water were used for cnh-cel sheet synthesis. A standard solution of HEC was prepared by dissolving 200 mg of cellulose in DI water. The cellulose nanofibers, when dissolved, can untangle or dissociate by subjecting them to ultra-sonication at a frequency of 23 kHz for 30 min. The cellulose solution was heated at 85 °C for 30 min to completely dissolve the cellulose fibers, which resulted in a transparent solution. CNHs were dispersed in DI water at loading concentrations of 10 mg, 20 mg, 50 mg, and 100 mg. The CNH solution was sonicated for 1 h. Initially, the CNHs precipitated due to their agglomeration and dahlia-like structures. When subjected to low-frequency ultra-sonication, an immediate dispersion was observed. The ratio of CNH to DI water was maintained at a very high rate, such that CNH exhibited enough room to disperse from their aggregated dahlia-like structures. Both solutions were divided into different portions depending on the ratios of HEC:CNH and then sonicated for 30 min to produce a volatile solution of different ratios of HEC:CNH which was agitated thoroughly. The combined solution was heated with stirring initially at 80 °C for 4 h at 200 rpm; to evaporate excess DI water, and the viscosity of the volatile solution started to increase. Subsequently, no excess DI water could be evaporated from the concentrated solution; the heat was raised to 90 °C for an hour and then finally to 100 °C. This resulted in a highly viscous, solution. The final solution was poured into a syringe, and a few droplets of this solution were dropped onto a clean glass plate to draw uniform sheets using the leveling applicator (bar coater). The sheets were allowed to dry at room temperature, and trapped a few molecules of water to maintain the structure. After a few minutes, the sheets were peeled off from the glass plate and analyzed using TEM, SEM, Raman, FTIR, as well as tensile strength, and conductance measurements, and the skin sensitization test. A schematic of the graphical representation of the Cnh-cel sheet, and its conductive path is shown in Fig. 1.

The skin sensitization test method is outlined as follows:

This study was conducted according to the OECD Guidelines for the Testing of Chemicals (OCED, 2016).

Cell culture

THP-1 cells were cultured in an incubator (37 °C and 5% CO_2) using RPMI-1640 supplemented with 10% fetal bovine serum (FBS), 0.05 mM 2-mercaptoethanol, 100 units/mL penicillin in 100 μg/mL streptomycin. The cells were seeded at a density of $0.1-0.2 \times 10^6$ cells/ mL once every 2 to 3 days to maintain a density of $0.1-1.0 \times 10^6$ cells/mL.

Determination of test dose

Three doses of working solutions were prepared as follows. Cnh-cel composites were added to the cell culture medium at a final concentration of 8,666 μg/mL. This working solution was serially diluted at 1:2 to prepare the remaining two working solutions. Eighty microliters of the cell suspension at a density of 2 $\times 10^6$ cells/mL was seeded into each well of a 96-well plate, and the cells were added with 80 μL working solutions or the medium (negative control) and cultured in an incubator for 24 h. Cells were then collected into 1.5 mL tubes and centrifuged at 250 × g, 4 °C, for 5 min. Cells were resuspended in 500 μL of FACS buffer (PBS supplemented with 0.1% BSA). After 10 washes with repetitive resuspension and

centrifugation, the cells were re-suspended in 200 μL FACS buffer. Immediately before measurement, the cells were stained by adding 5 μL propidium iodide (PI) (Invitrogen, Carlsbad, CA) solution (20 μg/mL diluted with FACS buffer). Cell viability was measured using flow cytometry, and the concentration (CV75) of the test sample in 75% cell viability was determined using Formula 1.

$$\text{Formula 1} \quad \log CV75 = \frac{(75 - c) \times log(b) - (75 - a) \times log(d)}{a - c}$$

a is the minimum value of cell viability over 75%

c is the maximum value of cell viability below 75%

b and **d** are the concentrations showing the value of cell viability **a** and **c**, respectively

Skin sensitization test

Four doses of Cnh-cel composite working solutions at concentrations of CV75 × $1.2^{-2, -1, 0, 1}$ were prepared. Cells were seeded, working solutions added, cultured, and washed as described above. After centrifugation, the cells were blocked with 330 μL of blocking solution (FACS buffer containing 0.01% human globulin Cohn fraction II, III for 15 min at 4 °C. The cells were divided into three tubes with 100 μl and added 30 μl of diluted anti-CD86, anti-CD54 or mouse IgG 1 antibodies. To make the diluted antibody solutions, the antibodies and FACS buffer were mixed at the ratios between antibody solutions and FACS buffer were at 6:44, 3:47, and 3:47, respectively. After 30 min at 4 °C, cells were washed with FACS buffer twice and re-suspended in 150 μL of FACS buffer followed by the addition of 4 μL of the diluted PI solution. The relative fluorescence intensity (RFI) was calculated using Formula 2 based on the measured mean fluorescence intensity (MFI) obtained by flow cytometry, as an indicator of CD86 and CD54 relative expression.

$$\text{Formula 2} \quad RFI = \frac{MFI \text{ of chemical treated cells} - MFI \text{ of chemical treated isotype control cell}}{MFI \text{ of vehicle control cells} - MFI \text{ of vehicle isotype control cells}} \times 100$$

Characterization:

JEOL JEM-2100F High-resolution Transmission electron microscopy was used at an operating voltage of 200 kV to capture images at high magnifications. A JEOL JSM 6060 LA scanning electron microscope was used to observe the surface morphology of the Cnh-cel sheets and different magnifications. For RAMAN analysis, a JASCO NRS-5100 Nps laser Raman spectroscope was used to characterize the structural fingerprint of molecules present in the Cnh-cel sheets. To understand the functional groups present in the composite sheets, JASCO FT-IR 4100 was used. Tensile strength measurement was

performed using a SHIMADZU AGS-X 5 N. Conductance of Cnh-cel sheets was measured using ADCMT 6423 DC voltage current source/monitor.

Results And Discussion

In vitro skin sensitization test

The results of the cytotoxicity and test dose determination tests are shown in Fig. 2. The CV 75 value was determined using Formula 1.

In this test, **a** = 89.5%, **b** = 1,083 μ/mL, **c** = 73.1%, **d** = 2,166 μg/mL. The CV75 value of Cnh-cel composites was 1,999 μg/mL. The exposure concentration of the Cnh-cel composites was set at four levels, diluted at a ratio of 1−2 based on CV75. The value were 2399 μg/mL (CV75 × 1.2), 1999 μg/mL (CV75), 1,666 μg/mL (CV75/1.2), 1,388 μg/mL (CV75/1.2^2).

The results of the skin sensitization tests are shown in Figs. 4 and 5. The results demonstrate that the RFI values of CD86 and CD54 are lower than the positive criteria (CD86 RFI ≥ 150, CD54 RFI ≥ 200). Therefore, Cnh-cel composites were identified as skin sensitization-negative in this experiment.

THP-1 cells were incubated with Cnh-cel composites (three doses: 4,333 μg/mL, 2,166 μg/mL, 1,083 μg/mL) or medium (negative control, 0 μg/mL) for 24 h. The cells were stained with PI solution. Cell viability was measured using flow cytometry.

THP-1 cells were incubated with Cnh-cel composites (four doses) for 24 h. The cells were stained with anti-CD86, anti-CD54, or mouse IgG-1 antibodies. MFI was measured using flow cytometry. RFI was calculated using MFI. The black bar represents the first result, and the white bar represents the second result. The Cnh-cel composites treated group showed that RFI values of CD86 and CD54 are lower than the positive criteria (CD86 RFI ≥ 150 and CD54 RFI ≥ 200). A working example of Cnh-cel sheets attached to human skin with glowing LED lights is shown in Fig. 6. Notably, these Cnh-cel sheets did not exhibit skin sensitization in other bioassays, such as OECD TG442C (Amino acid Derivative Reactivity Assay) or OECD TG442D (data included in Supplementary Information).

Transmission Electron Microscopy

To investigate the interparticle interaction between the CNH aggregates, a transmission electron microscope was employed. Pristine carbon nanohorn samples were prepared by sonicating pristine samples in ethanol and DI water, and drop-casting on a copper grid.

Similarly, cellulose samples doped with CNHs were diluted with DI water and drop-cast on to the copper grid and dried on a hot plate for a few minutes. As shown in the TEM images in Figs. 7(a) and 7(b), the pristine samples of CNH have cone-like structures, with single and double-walled CNHs arranged in dahlia-like structures, with the conical tip prodding out of the dahlia-like assembly. The pristine CNHs

have cone tips of 2–3 nm in thickness. Figure 7(c) shows that these dahlia-like structures are accompanied by a layer of cellulose coating on the outer side connecting adjacent dahlia-like structured CNHs. This shows that the cellulose has adhered both in between and on top of the conical tips of the CNHs. As shown in Fig. 7(d), a distorted ring-like structure of amorphous carbon surrounding the dahlia-like structures, can be seen when magnified at 50 nm using TEM.

Scanning electron microscopy

Scanning electron microscopy of the Cnh-cel sheets is shown in Figs. 8(a) − 8(d). The Cnh-cel sheets are observed under SEM at an accelerating voltage of 5 kV. The morphology of the Cnh-cel sheets determine various parameters about the Cnh-cel sheets.

Raman spectroscopy

Raman spectroscopy characterization is a useful method of analysis to evaluate the purity of carbon nanomaterials. As interpreted from the plot in Fig. 9, CNHs exhibit two bands at 1,338 cm^{-1} (D band) and 1,580 cm^{-1} (G-band) (32).

Fourier Transform Infrared Spectroscopy

FTIR analysis of Cnh-cel sheets revealed the presence of a variety of functional groups in the Cnh-cel sheets. All the different loading concentrations of Cnh-cel sheets have a similar type of functional group fingerprint, as shown in Fig. 10.

Tensile strength measurement

Tensile strength measurement is a crucial component in determining the durability and strength of the sheets. As the CNH loading increases, the strength decreases as the CNHs loading reduces the interparticle bonding between the adjacent cellulose molecules. The CNH loading concentration of 10 mg had a displacement of 3.074 mm having an ultimate strength to withstand a force of 1001.50 mN, as shown in Fig. 11. In contrast, the 20 mg loading was able to withstand a displacement of 1.62 mm but had an ultimate strength to tolerate a force of 990.7 mN until they broke. This shows that when the loading concentration is doubled, and the displacement was reduced by 52.7%, but the ultimate strength was only affected by 9.8%. Similarly, at 50 mg loading, the displacement was 1.2 mm at which it could stand 865.79 mN of force, whereas for 100 mg loading the displacement was 0.23 mm for the ultimate strength to bear the force of 164.24 mN.

Conductance measurement

A typical measurement of conductance for sheets is determined by its area of cross-sectional area and length. However, the conductance varies with the variation in the length and thickness of sheets. By keeping the parameters of length and thickness to a certain roundoff, the conductance is determined. The conductance measurements are proportional to the level of doping of CNH in the cellulose matrix as the CNH doping increases the conductance of the sample by 100%. However, we could not determine the maximum doping possible to retain the geometry of the thin film for < 100 μm sized sheets at 50 wt% cellulose. Figure 13 shows the combined plot of the voltage (V) vs. current (I), however, the current values are different for all the Cnh-cel sheets.

Discussion

The present report on Cnh-cel composite sheets and its test for skin compatibility test is the first report and there is not history of any previous reports for this study available according to our literature survey.

In vitro skin sensitization test the concentration of Cnh-cel composites and cell viability were inversely proportional (Fig. 3). Thus, a high concentration of Cnh-cel composites is cytotoxic. The CV75 value of the Cnh-cel composite was 1999 μg/mg. The CV75 value of lactic acid, which is used in cosmetics suggests a relatively low cytotoxicity value of 1000 μg/mL. Given the comparison of the CV75 values, the cytotoxicity of the Cnh-cel composites is relatively low.

In the transmission electron microscopy, the interaction between the long chains of cellulose nanofibers and the carbon nanohorns can be observed in the TEM images. Therefore, it can be concluded that even without any surface modification of the CNHs, interactions between CNHs and cellulose can be achieved. It is also observed that each dahlia-like aggregate of CNHs has a uniformly layered covering of cellulose; showing all the virtuous composites of cellulose and CNHs. This covering of cellulose to the CNH aggregates makes the CNHs aggregate as core-shell type nanoparticles, which can also be used in other applications where dissociation of the CNHs is not necessary and the dahlia-like structure is kept intact while allowing the CNHs to interact with other molecules via the cellulose shell. The interaction between the CNHs and cellulose can also be confirmed by FTIR analysis.It is seen in the SEM images that, as the CNH loading concentration increase, the smoothness of the surface of the Cnh-cel sheets changes gradually. With the 100 mg doping concentration of CNH shown in Fig. 8(d), the surface morphology of the Cnh-cel sheet is rough and porous compared to the 10 mg doping, as shown in Fig. 8 (a). In addition, as in Fig. 8 (b) and 8 (c), the CNH doping concentrations are 20 mg and 50 mg, respectively, and the surface morphology is greatly varied. This indicates that the cellulose concentration in the Cnh-cel sheets is responsible for the surface smoothness and strength, as confirmed using the tensile strength measurement. In conclusion, the magnified images of the surface of the Cnh-cel sheets show that the strength and conductance are inversely related to the concentration of the cellulose and CNHs.

Raman spectroscopy The D band is observed because of the sp^3 carbon, which produces elastic scattering. The intensities of I_d and I_g correspond to the sp^3 and sp^2 hybridization of carbon atoms present in the CNHs (I_d/I_g= 1.2). For pristine CNH, the D band is significantly higher than that of 10 mg

CNH-doped sheet. The presence of D and G bands confirm the presence of CNHs in the Cnh-cel sheets. The increase in the Raman intensities corresponds to the increase in the CNH loading concentration but not in exact proportion to the loading concentration. In the Fourier transform Infrared spectroscopy, it is a well-known fact that the cellulose is a hygroscopic material, hence few bonds are related to the hygroscopic property, and OH$^-$ bonds are detected at 3,340 cm^{-1} also involving weak stretching at 2,896 cm^{-1}, both of which explain the hygroscopic nature of cellulose. Furthermore, an absorption band at 1,065 cm^{-1} corresponding to the $^-$(COH) functional group was also observed, and also a COO functional group is was identified at 1,562 cm^{-1}.

In the tensile strength of Cnh-cel sheets, threshold of the force endurable for Cnh-cel sheets for pristine Cnh-cel composite are collectively plotted in CNH loading versus force, and the displacement is shown below in Fig. 11. The plot shows a trend of a decrease by the force and displacement proportional to the loading concentration, which enables us to understand the suitable loading concentrations based on the type of application. It was found that a further increase in the loading concentration of CNHs could not provide structural integrity to fabricate thin films of less than 100 μm in thickness, which could be related to the upper limit of doping, possibly for pristine CNHs to cellulose ratios. However, functionalization of the CNHs and dissolving the cellulose in ionic liquids (33) could increase the endurance of Cnh-cel composite sheets, while compromising other properties. A typical setup of the tensile strength measurement of a Cnh-cel sheet is shown in Fig. 12. In the conductance measurement, the conductance of the sheets with 10 mg and 20 mg loading of CNHs show a non-linear V-I curve, which indicates that the sheets are not good conductors, and the conductance cannot be determined as the sheets do not have a linear V-I curve. However, at 50 and 100 mg loading of CNHs, a linear V-I curve is observed, which translates to a conductance of 6.145×10^{-6} S for 50 mg loading and 1.88×10^{-5} S for 100 mg loading.

Conclusion

Cellulose carbon nanohorn composite sheets (Cnh-cel sheets) with different loading concentrations were successfully fabricated in our study. The properties of the Cnh-cel sheets were analyzed and determined using various characterization techniques. The conductance of the Cnh-cel sheet at the maximum loading concentration was measured to be 1.88×10^{-5} S, and the skin application of the Cnh-cel sheets to human skin was also tested, and it was proven to be safe for applications on human skin. These initial experiments of Cnh-cel sheets shed light on the understanding of carbon allotropes application as smart materials. The encouraging properties of Cnh-cel sheets such as flexibility, strength, conductive, and skin-compatible indicate their high potential for various modern-day applications.

Abbreviations

HEC: Hydroxyethylcellulose (HEC)

CNH: Carbon nanohorn

CNT: Carbon nanotube

h-CLAT: Human cell line activation

SWCNTs: single-walled carbon nanotubes

TEM: Transmission electron microscopy

SEM: Scanning electron microscopy

FTIR: Fourier transform infrared spectroscopy

Declarations

Acknowledgment

The author thanks SGU-MEXT for their support for pursuit of a Ph.D. in Japan.

Author's contributions

K.P.S. performed the experiment of the Cnh-cel sheets, T.N., and K.K. performed the skin cell test of the Cnh-cel sheets, M.K., and T.K. analyzed the data, Y.N. drafted the manuscript, N.T supervised the experiment A.S. and Y.H. provided the materials.

Funding

This work was supported by Okayama Prefecture Industrial promotion grant, "Toku-den" (T.N., A.S., Y.H.). This work is supported in part by MEXT/JSPS KAKENHI grant numbers 18K06133 (AS), 17H03818 (YN).

Availability of data and materials

All data generated and analyzed during the current study are available with the corresponding author upon reasonable request.

Ethics approval and consent to participate

This study does not require any formal consent as it does not include any human participation or animal experimentation.

Consent for publication

Not applicable.

Competing interests

The authors declare that they have no competing interest.

References

1. Hoyos-Palacio LM, García AG, Pérez-Robles JF, González J, Martínez-Tejada H V. Catalytic effect of Fe, Ni, Co and Mo on the CNTs production. IOP Conf Ser Mater Sci Eng. 2014;59(1).

2. Osorio AG, Silveira ICL, Bueno VL, Bergmann CP. H2SO4/HNO3/HCl-Functionalization and its effect on dispersion of carbon nanotubes in aqueous media. Appl Surf Sci. 2008;255(5 PART 1):2485–9.

3. Vaisman L, Wagner HD, Marom G. The role of surfactants in dispersion of carbon nanotubes. Adv Colloid Interface Sci. 2006;128–130(2006):37–46.

4. Iijima S, Yudasaka M. sdarticle_Iijima_nanohorn_CPL.pdf. 1999;(August):165–70.

5. Cioffi C, Campidelli S, Sooambar C, Marcaccio M, Marcolongo G, Meneghetti M, et al. Synthesis, characterization, and photoinduced electron transfer in functionalized single wall carbon nanohorns. J Am Chem Soc. 2007;129(13):3938–45.

6. Ajima K, Yudasaka M, Murakami T, Maigné A, Shiba K, Iijima S. Carbon nanohorns as anticancer drug carriers. Mol Pharm. 2005;2(6):475–80.

7. Kadambi SB, Pramoda K, Ramamurty U, Rao CNR. Carbon-Nanohorn-Reinforced Polymer Matrix Composites: Synergetic Benefits in Mechanical Properties. ACS Appl Mater Interfaces. 2015;7(31):17016–22.

8. Kroschwitz JI, Seidel A. Kirk-Othmer encyclopedia of chemical technology. Volumes 1, 5th edition

9. Lerk CF, Lagas M, Fell JT, Nauta P. Effect of Hydrophilization of Hydrophobic Drugs on Release Rate from Capsules. J Pharm Sci. 1978 Jul 1;67(7):935–9.

10. Qi H, Liu J, Pionteck J, Pötschke P, Mäder E. Carbon nanotube-cellulose composite aerogels for vapour sensing. Sensors Actuators, B Chem. 2015;213:20–6. http://dx.doi.org/10.1016/j.snb.2015.02.067

11. Qi H, Mäder E, Liu J. Unique water sensors based on carbon nanotube-cellulose composites. Sensors Actuators, B Chem. 2013;185:225–30. http://dx.doi.org/10.1016/j.snb.2013.04.116

12. Gao K, Shao Z, Wu X, Wang X, Li J, Zhang Y, et al. Cellulose nanofibers/reduced graphene oxide flexible transparent conductive paper. Carbohydr Polym. 2013;97(1):243–51. http://dx.doi.org/10.1016/j.carbpol.2013.03.067

13. Choi HY, Lee TW, Lee SE, Lim JD, Jeong YG. Silver nanowire/carbon nanotube/cellulose hybrid papers for electrically conductive and electromagnetic interference shielding elements. Compos Sci Technol. 2017;150:45–53. http://dx.doi.org/10.1016/j.compscitech.2017.07.008

14. Zhao D, Zhang Q, Chen W, Yi X, Liu S, Wang Q, et al. Highly Flexible and Conductive Cellulose-Mediated PEDOT:PSS/MWCNT Composite Films for Supercapacitor Electrodes. ACS Appl Mater Interfaces. 2017;9(15):13213–22.

15. GHS (Rev.7) (2017) - Transport - UNECE. https://www.unece.org/trans/danger/publi/ghs/ghs_rev07/07files_e0.html

16. Organisation for Economic Co-operation and Development. The Adverse Outcome Pathway for Skin Sensitisation Initiated by Covalent Binding to Proteins. OECD Publishing; 2014. 105 p.

17. Organisation for Economic Co-operation and Development. Skin sensitisation. OECD Publishing; 1992. 9 p.

18. Organisation for Economic Co-operation and Development. 429. Skin sensitization : local lymph node assay. OECD Publishing; 2010. 20 p.

19. Ban on Animal Testing | Internal Market, Industry, Entrepreneurship and SMEs. https://ec.europa.eu/growth/sectors/cosmetics/animal-testing_en

20. In chemico skin sensitisation : direct peptide reactivity assay (DPRA). 19 p.

21. Gerberick GF, Vassallo JD, Bailey RE, Chaney JG, Morrall SW, Lepoittevin J-P. Development of a Peptide Reactivity Assay for Screening Contact Allergens. Toxicol Sci. 2004 Jul 14;81(2):332–43. https://academic.oup.com/toxsci/article-lookup/doi/10.1093/toxsci/kfh213

22. Test No. 442C: In Chemico Skin Sensitisation. OECD; 2019 (OECD Guidelines for the Testing of Chemicals, Section 4). https://www.oecd-ilibrary.org/environment/test-no-442c-in-chemico-skin-sensitisation_9789264229709-en

23. Gerberick GF, Vassallo JD, Foertsch LM, Price BB, Chaney JG, Lepoittevin J-P. Quantification of Chemical Peptide Reactivity for Screening Contact Allergens: A Classification Tree Model Approach. Toxicol Sci. 2007 Jan 18;97(2):417–27. https://academic.oup.com/toxsci/article-lookup/doi/10.1093/toxsci/kfm064

24. Emter R, Ellis G, Natsch A. Performance of a novel keratinocyte-based reporter cell line to screen skin sensitizers in vitro. Toxicol Appl Pharmacol. 2010 Jun 15;245(3):281–90. https://www.sciencedirect.com/science/article/pii/S0041008X10000955?via%3Dihub

25. Natsch A. The Nrf2-Keap1-ARE Toxicity Pathway as a Cellular Sensor for Skin Sensitizers—Functional Relevance and a Hypothesis on Innate Reactions to Skin Sensitizers. Toxicol Sci. 2010 Feb 1;113(2):284–92. https://academic.oup.com/toxsci/article/1674730/The

26. Organisation for Economic Co-operation and Development. In vitro skin sensitisation : ARE-Nrf2 luciferase test method. 20 p.

27. TG 495: Ros (Reactive Oxygen Species) Assay for Photoreactivity. OECD; 2019. (OECD Guidelines for the Testing of Chemicals, Section 4). https://www.oecd-ilibrary.org/environment/tg-495-ros-reactive-oxygen-species-assay-for-photoreactivity_915e00ac-en

28. Test No. 442D: In Vitro Skin Sensitisation. OECD; 2018. (OECD Guidelines for the Testing of Chemicals, Section 4). Available from: https://www.oecd-ilibrary.org/environment/test-no-442d-in-vitro-skin-sensitisation_9789264229822-en

29. Organisation for Economic Co-operation and Development. Test No. 442E: In Vitro Skin Sensitisation : Human Cell Line Activation Test (h-CLAT). OECD Publishing; 2016. 21 p.

30. Ashikaga T, Yoshida Y, Hirota M, Yoneyama K, Itagaki H, Sakaguchi H, et al. Development of an in vitro skin sensitization test using human cell lines: The human Cell Line Activation Test (h-CLAT). Toxicol Vitr. 2006 Aug;20(5):767–73. http://www.ncbi.nlm.nih.gov/pubmed/16311011

31. Aiba S, Terunuma A, Manome H, Tagami H. Dendritic cells differently respond to haptens and irritants by their production of cytokines and expression of co-stimulatory molecules. Eur J Immunol. 1997 Nov;27(11):3031–8. http://www.ncbi.nlm.nih.gov/pubmed/9394834

32. Lin Z, Iijima T, Karthik PS, Yoshida M, Hada M, Nishikawa T, et al. Surface modification of carbon nanohorns by helium plasma and ozone treatments. Jpn J Appl Phys. 2017 Jan 1;56(1S):01AB08.

33. Zhao D, Fu L, Zhang J, Li H, Liu M, Fu J, et al. Study on the Dissolution of Cellulose in <I>N</I>-Allylpyridinium Chloride Ionic Liquid and Co-Solvent Composites. Acta Polym Sin. 2012;012(9):937–42.

Figures
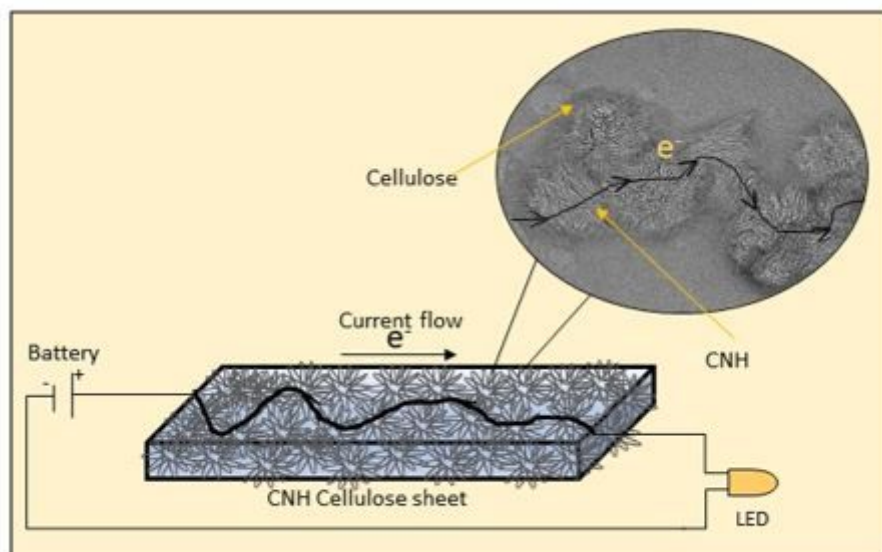
Figure 1

Graphical representation of a conductive path in the CNH-cellulose sheet
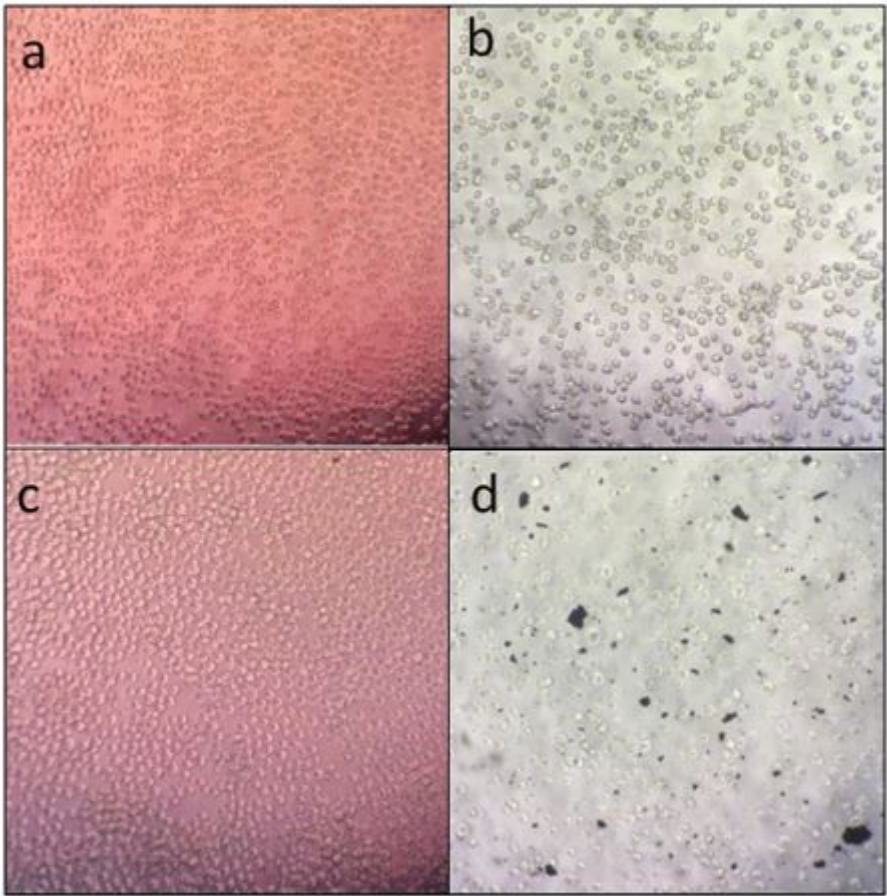
Figure 2

(a) Initial media control (b) Media control (incubate 24 h) (c) Media control (after centrifugation) (d) Cnh-Cell sheets (after centrifugation)
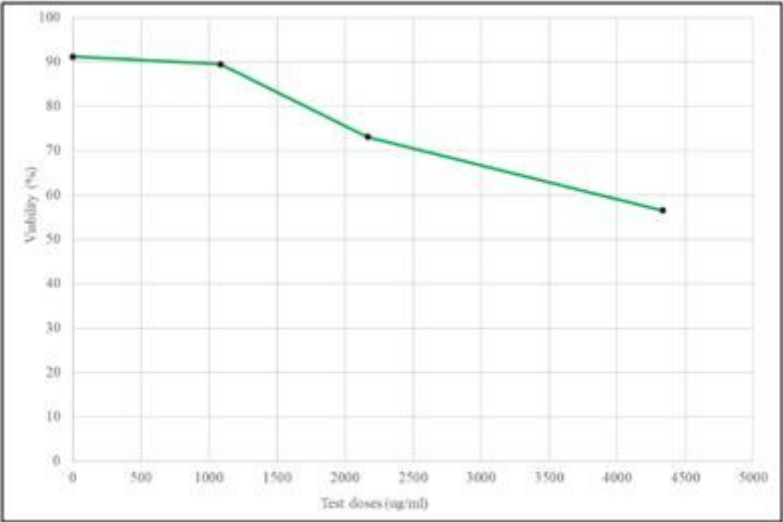
Figure 3

Cell viability effects of three test doses
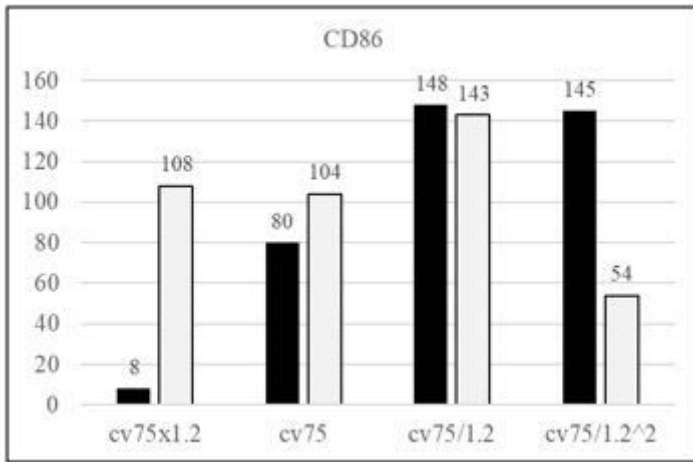
Figure 4

RFI data for CD86
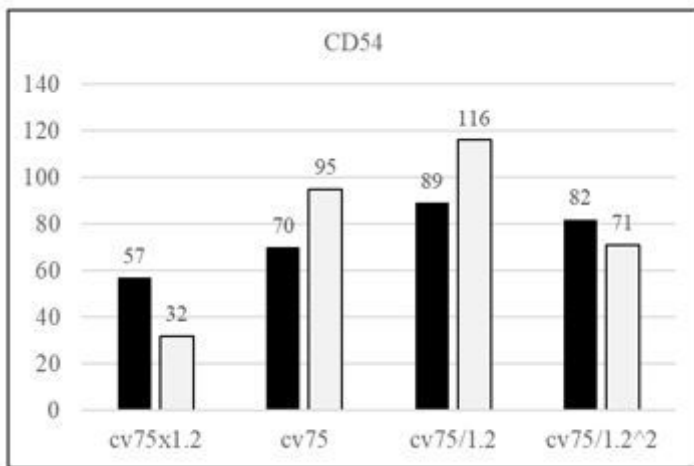
Figure 5

RFI data for CD54
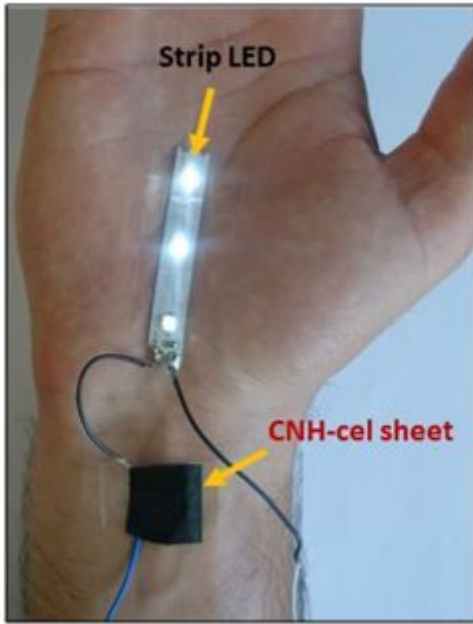
Figure 6

The application of Cnh-cel sheets on human skin and passage an electric current to light up LEDs
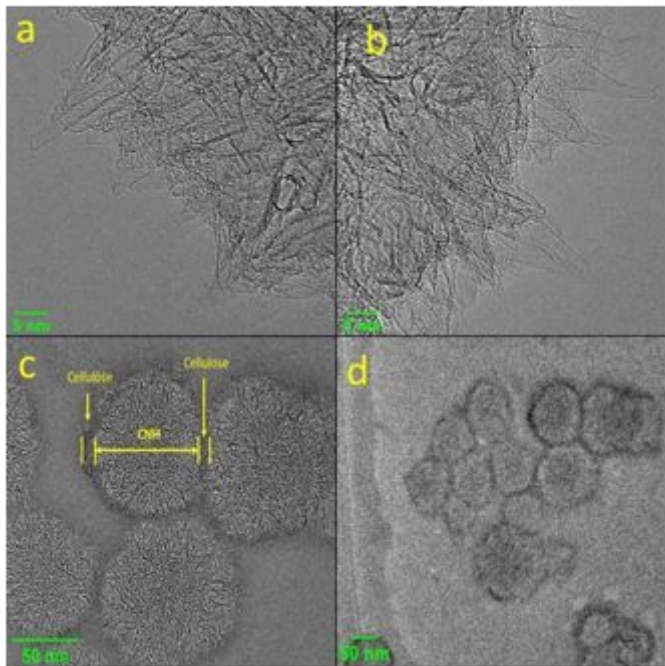
Figure 7

Pristine CNHs (a) and (b) observed under TEM (c) and (d), showing the interaction of cellulose and CNHs
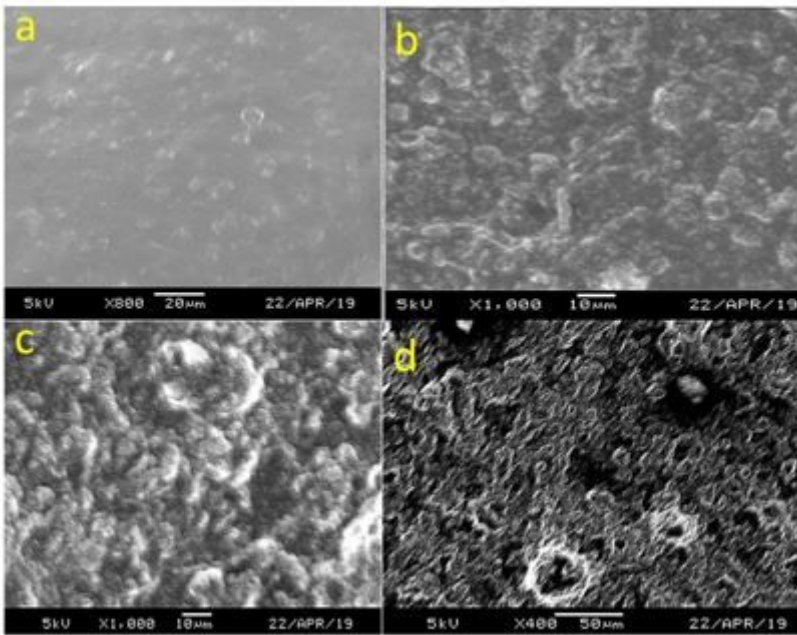
Figure 8

SEM images at different loading concentrations of CNH (a) 10 mg, (b)20 mg, (c) 50 mg, (d)100 mg
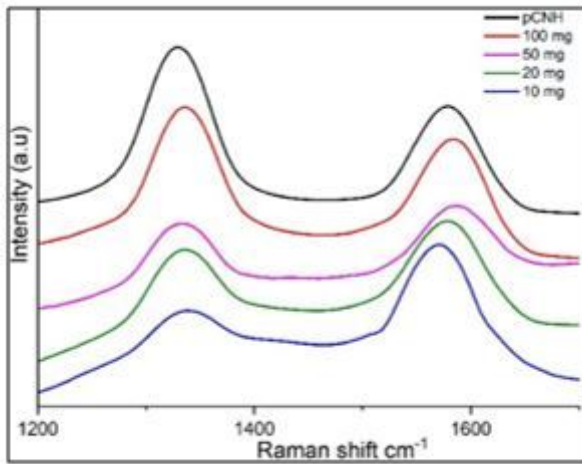
Figure 9

Raman plot of CNH-cel sheets
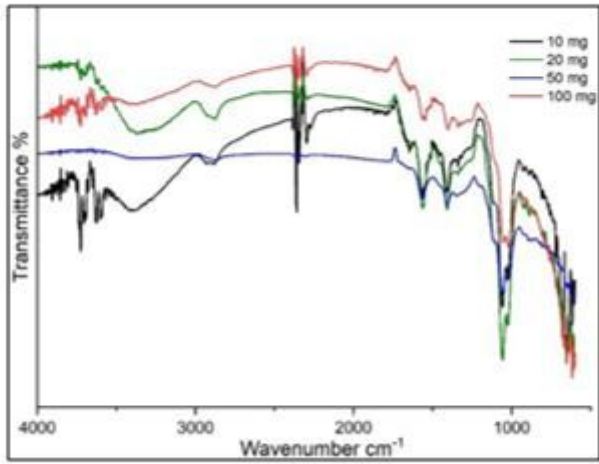
Figure 10

FT-IR plot of CNH-cel sheets
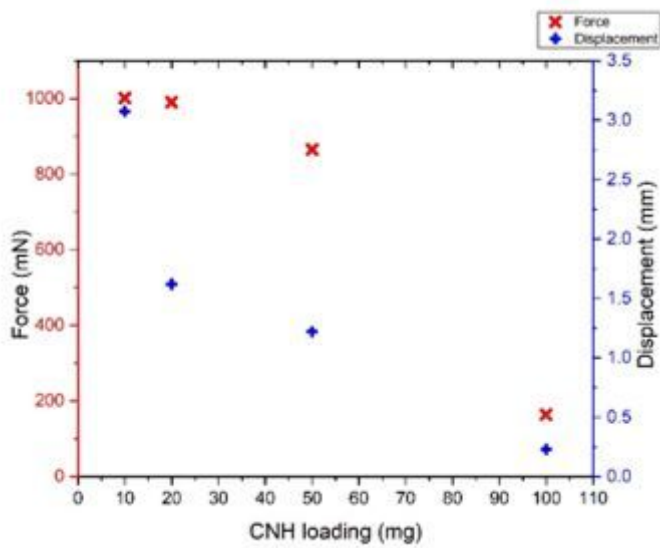
Figure 11

Tensile strength measurement of the Cnh-cell sheets
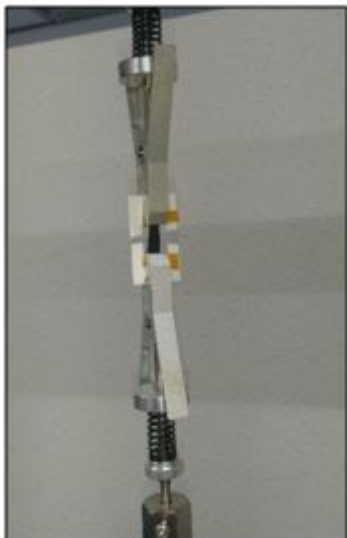
Figure 12

Cnh-cel sheet tensile measurement setup
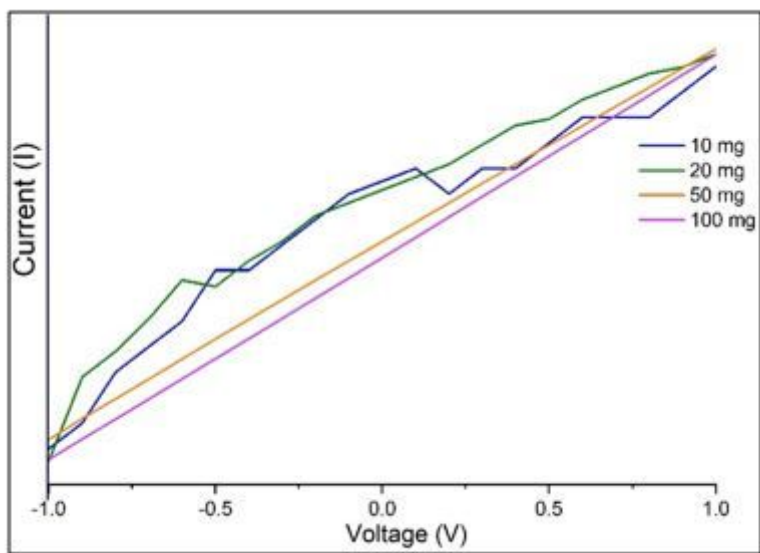
Figure 13

V-I curve of Cnh-cel sheets